Preparation of Nanocrystalline Molybdenum Disilicide ($MoSi_2$) by a Chlorine-Transfer Reaction

Timothy J. Trentler,† R. Suryanarayanan Iyer,‡ Shankar M. L. Sastry,‡ and William E. Buhro*,†

Departments of Chemistry and Mechanical Engineering, Washington University, St. Louis, Missouri 63130-4899

Received March 27, 2001. Revised Manuscript Received July 10, 2001

Reaction of $MoCl_3$ and Si at 500 °C produces phase-pure $MoSi_2$ powders in near-quantitative yields. Use of an inert diluent (LiCl or $ZnCl_2$) enables the production of nanocrystalline powders. The diluent can be subsequently removed by washing with methanol or by sublimation. Consolidation of diluent-free powders by hot pressing at 1400 °C and 375 MPa for 0.5−4 h affords dense compacts (>95% theoretical density) possessing nanocrystalline grains (<50 nm) and exhibiting hardnesses of 15.0−16.3 GPa. This constitutes a 60−75% enhancement in hardness over conventional, microcrystalline $MoSi_2$.

Introduction

Herein we describe a synthesis of $MoSi_2$ that generates nanocrystalline powders, which are subsequently consolidated to dense nanocrystalline compacts. The intermetallic compound $MoSi_2$, commonly employed in high-temperature heating elements, is a candidate structural material for aerospace applications because of its strength, oxidation resistance, and low density.[1,2] Brittleness and low creep resistance in conventional coarse-grained (microcrystalline) $MoSi_2$, however, render it unsuitable for many applications.[1,2] Introduction of reinforcements in $MoSi_2$ to form composites and $MoSi_2$ alloying have produced substantial improvements in mechanical properties.[1,2] Grain-size engineering—specifically, reduction of grain sizes into the nanometer regime—offers another potentially useful way for optimizing the properties of $MoSi_2$.

In nanocrystalline materials grain boundaries rather than dislocations govern mechanical behavior,[3−5] resulting in mechanical properties that are dramatically altered from those of conventional coarse-grained materials.[6,7] Nanocrystalline ceramics[3,8−11] and intermetallics[12] become ductile or even superplastic, and nanocrystalline metals[13,14] become exceptionally strong. Similar property enhancements might be expected of nanocrystalline $MoSi_2$.

Fabrication of nanocrystalline $MoSi_2$, however, is hindered by the limited preparative chemistries available. Bulk $MoSi_2$ is typically prepared by metallothermic reductions (eq 1),[15,16] or by direct reaction of the elements, which has been accomplished by innumerable methods.[17] Few alternative reactions have appeared in the literature; among them are a solid-state metathesis reaction (eq 2)[18] and transfer of carbon (or oxygen) in the solid state from molybdenum to silicon (eq 3).[19] These methods require high energy inputs (resulting in large grains) and/or yield byproducts that are inconvenient to remove.

$$MoO_3 + 2Si + 3Mg \rightarrow MoSi_2 + 3MgO \quad (1)$$

$$8MoCl_5 + 10Mg_2Si \rightarrow 5MoSi_2 + 20MgCl_2 + 3Mo \quad (2)$$

$$Mo_2C + 3Si \rightarrow MoSi_2 + SiC \quad (3)$$

We previously reported a low-temperature, solution-based variant of the reductive syntheses, which implements sonochemical agitation (eq 4).[20]

* To whom correspondence should be addressed. E-mail: buhro@wuchem.wustl.edu.
† Department of Chemistry.
‡ Department of Mechanical Engineering.

(1) Vasudevan, A. K.; Petrovic, J. J. *Mater. Sci. Eng.* **1992**, *A155*, 1.
(2) Petrovic, J. J. *MRS Bull.* **1993**, *18*, 35.
(3) Karch, J.; Birringer, R.; Gleiter, H. *Nature* **1987**, *330*, 556.
(4) Siegel, R. W. *MRS Bull.* **1990**, *15*, 60.
(5) Gryaznov, V. G.; Trusov, L. I. *Prog. Mater. Sci.* **1993**, *37*, 289.
(6) Suryanarayana, C.; Froes, F. H. *Adv. Mater.* **1993**, *5*, 96.
(7) Bohn, R.; Haubold, T.; Birringer, R.; Gleiter, H. *Scr. Metall. Mater.* **1987**, *25*, 811.
(8) Niihara, K. *J. Ceram. Soc. Jpn.* **1991**, *99*, 975.
(9) Vassen, R.; Stover, D. *J. Mater. Proc. Technol.* **1999**, *93*, 77.
(10) Yan, D. S.; Zheng, Y. S.; Gao, L.; Zhu, C. F.; Wang, X. W.; Bai, C. L.; Xu, L.; Li, M. Q. *J. Mater. Sci.* **1998**, *33*, 2719.
(11) Mayo, M. J.; Hague, D. C.; Chen, D.-J. *Mater. Sci. Eng.* **1993**, *A166*, 145.
(12) McFadden, X.; Mishra, R. S.; Valiev, R. Z.; Zhilyaev, A. P.; Mukherjee, A. K. *Nature* **1999**, *398*, 684.
(13) Nieman, G. W.; Weertman, J. R.; Siegel, R. W. *Scr. Metall.* **1990**, *24*, 145.
(14) Nieman, G. W.; Weertman, J. R.; Siegel, R. W. *Scr. Metall.* **1989**, *23*, 2013.
(15) Killeffer, D. H.; Linz, A. *Molybdenum Compounds*; Interscience: New York, 1952.
(16) Ambramovici, R.; Hida, G. T. U.S. Patent 5 011 800, 1991.
(17) Jeng, Y.-L.; Lavernia, E. J. *J. Mater. Sci.* **1994**, *29*, 2557.
(18) Jacubinas, R. M.; Kaner, R. B. *Mater. Res. Soc. Symp. Proc.* **1994**, *322*, 133.
(19) Zeng, D.; Hampden-Smith, M. J.; Wang, L. M. *J. Mater. Chem.* **1993**, *3*, 777.
(20) Trentler, T. J.; Suryanarayanan, R.; Sastry, S. M. L.; Buhro, W. E. *Mater. Sci. Eng.* **1995**, *A204*, 193.

10.1021/cm010267c CCC: $20.00
Published on Web 09/13/2001

$$MoCl_5 + 2SiCl_4 + {}^{13}/_2NaK \xrightarrow[\text{hexane}]{)))))} MoSi_2 + {}^{13}/_2NaCl + {}^{13}/_2KCl \quad (4)$$

This preparation and the mechanical milling (also known as mechanical attrition or high-energy ball milling) of coarse-grained $MoSi_2$ powders[21] or Mo/Si mixtures[22−24] are the only methods reported to date that yield nanocrystalline $MoSi_2$. However, neither the mechanical-milling synthesis nor the sonochemical synthesis is ideal. The sonochemical preparation incorporated large quantities of carbonaceous impurities from the solvent.[25] Mechanical milling introduced nitride, oxide, and iron impurities from adventitious air exposure and the steel milling balls.[21] Additionally, the milled powders consisted of large micrometer-sized particles having nanocrystalline fine structure,[21] as is typical of milled powders,[26] which can be difficult to consolidate to full density.[27]

We now report the synthesis of $MoSi_2$ by a reaction analogous to eq 3, but with chlorine as the displaced element (eq 5).

$$4MoCl_3 + 11Si \rightarrow 4MoSi_2 + 3SiCl_4 \quad (5)$$

$$[\Delta H_{298} = -62.0 \text{ kcal/(mol of } MoSi_2)]$$

This reaction is quite exothermic, has a low activation barrier, and generates a volatile byproduct, $SiCl_4$. Incorporation of an inert diluent into the reaction mixture affords control of the mean particle size and thereby enables the formation of nanocrystalline powders. These powders are successfully consolidated via hot pressing to high density with retention of nanocrystalline grain sizes.

Experimental Section

General Procedures. All reactions were conducted in a Lindbergh Blue M tube furnace under argon. Reaction mixtures were prepared and products collected under N_2. $MoCl_3$ (Alfa-Aesar, 99.5%), Si (1−5 μm, Alfa-Aesar, 5 N), LiCl (Aldrich, 99%), and $ZnCl_2$ (Aldrich, 98%) powders were used as received.

X-ray diffraction (XRD) data were collected on a Rigaku DmaxA diffractometer and were analyzed using Materials Data, Inc. software. JCPDS reference patterns were used for identification of crystalline phases. Coherence lengths were calculated using the JADE X-ray powder data processing program. Reported coherence lengths for α-$MoSi_2$ correspond to the average of the values calculated from the four strongest reflections appearing below $50° = 2\theta$. For β-$MoSi_2$, the coherence length calculated from the 100% reflection is given.

Transmission electron microscopy (TEM) was performed on a JEOL 2000 FX microscope operating at 200 keV. Elemental compositions were determined via energy-dispersive X-ray spectroscopy (EDS) using a Noran Voyager X-ray spectrometer. TEM specimens were prepared on Cu grids covered with a holey carbon film. Scanning electron microscopy (SEM) was performed on a Hitachi S-4500 field-emission instrument equipped with a Noran Instruments Voyager II X-ray quantitative microanalysis system (EDS).

^{29}Si NMR spectra were obtained on a Varian XL-300 spectrometer.

Mechanical properties were determined by microindentation. Vickers hardness numbers (VHNs) were determined under an indentation load of 200 g, and the average of at least 10 indents is reported. Fracture toughness values (K_{Ic}) were calculated by the method of Antis[28] from crack lengths that emanated from indents under application of a 1 kg load.

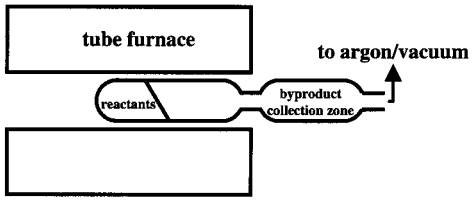

Figure 1. Diagram of the reaction vessel. The constriction minimizes blowout of the reactants and products.

Preparation of $MoSi_2$ from $MoCl_3$ and Si. This reaction was conducted on several scales, and the procedure described here is for an 8 g theoretical yield of $MoSi_2$. $MoCl_3$ (10.76 g, 53.19 mmol) and Si (4.111 g, 146.4 mmol) were thoroughly mixed in a mortar until the powder was homogeneous in appearance. This mixture was added to a fused-silica tube that possessed a reaction zone (1 in. diameter) and a byproduct collection zone (1 in. diameter) separated by a constricted zone (1/4 in. diameter, 3 cm long). The tube was connected to an argon line equipped with a bubbler to prevent a pressure buildup, and was inserted into a tube furnace with the constriction situated at the opening (Figure 1). The mixture was heated under argon with a ramp rate of 20 °C/min to 500 °C. A soak time of 5 min was adequate for completing the reaction. The reaction tube was allowed to cool, and then a colorless byproduct liquid that condensed in the collection zone of the tube was stripped in vacuo. A dark gray product that was analyzed as α-$MoSi_2$ by XRD was collected (7.59 g, 49.90 mmol, 94% yield). *Warning! This is an exothermic reaction that could become violent if conducted on very large scales.*

Preparation of $MoSi_2$ with Added Diluent. These reactions were conducted analogously to that above, but with an inert salt (LiCl or $ZnCl_2$) intermixed with the reactants. The diluent:$MoCl_3$ molar ratio was varied from 0.5 to 10. The typical reaction was conducted with 3.27 g (16.2 mmol) of $MoCl_3$ and 1.25 g (44.4 mmol) of Si. The diluent salt was removed after the reaction by sublimation under dynamic vacuum (10^{-3} Torr) at 500 °C ($ZnCl_2$) or 750−900 °C (LiCl), or by washing with MeOH under an atmosphere of N_2 (the latter method was used for samples that were consolidated as described below). The mass yields were ca. 98%, but the products of many trials required further annealing to complete the formation of $MoSi_2$ (see the Results and Discussion).

Consolidation of Nanocrystalline Powders. Nanocrystalline powders (3.75−6.00 g) prepared in the presence of a diluent (2.5:1 LiCl/$MoCl_3$) were consolidated by uniaxial hot pressing in an argon-filled drybox. A two-piece die with an outer cylinder of TZM alloy (composition $Mo_{46}Ti_{45}Zr_7C_2$) and an inner sleeve of graphite and having an internal cross section of 13 mm was used. An initial load of 175 MPa was applied to the cold powders. This load was maintained until the desired set-point temperature was reached, at which time the pressure was increased (see Table 1 the for parameters). After a desired time period, the pressure was released to ∼20 MPa, and then the temperature was ramped down at a rate of ∼200 °C/h (to avoid macrocracking that occurred with faster cooling). The resultant compacts were polished and then surface etched (HF/HNO_3/lactic acid, 10:30:60). The compact density was deter-

(21) Haji-Mahmood, M. S.; Chumbley, L. S. *Nanostruct. Mater.* **1996**, *7*, 95.
(22) Fei, G. T.; Liu, L.; Ding, X. Z.; Zhang, L. D.; Zheng, Q. Q. *J. Alloys Compd.* **1995**, *229*, 280.
(23) Gaffet, E.; Malhouroux-Gaffet, N. *J. Alloys Compd.* **1994**, *205*, 27.
(24) Tan, Q.; Zangvil, A. *J. Mater. Res.* **1999**, *14*, 2701.
(25) Trentler, T. J. Ph.D. Dissertation, Washington University, St. Louis, MO, 1997; p 200.
(26) Koch, C. C. *Nanostruct. Mater.* **1993**, *2*, 109.
(27) Mayo, M. J. *Int. Mater. Rev.* **1996**, *41*, 85.
(28) Antis, G. R.; Chantikul, P.; Lawn, B. R.; Marshall, D. B. *J. Am. Ceram. Soc.* **1981**, *64*, 533.

Table 1. $MoSi_2$ Powder Consolidation and Compact Structure, Composition, and Properties

powder sample	phases[a] present in the powder prior to consolidation	crystallite size[b] (nm)	heating, pressing, and cooling times (h)	pressing T, P (°C, MPa)	phases[a] present in the compact after consolidation	grain size[b] (nm)	ρ (%)[c]	VHN[d] (GPa)	K_{Ic}[e] (MPa $m^{1/2}$)
1	β-$MoSi_2$, Mo, Si, Mo_3Si	<20	1.0, 0.5, 0.3	1400, 375	α-$MoSi_2$	40	>90[f]	12.5	4.0
1	β-$MoSi_2$, Mo, Si, Mo_3Si	<20	1.3, 4.0, 0.3	1400, 375	α-$MoSi_2$	32	>95[f]	15.0	4.8
2	β-$MoSi_2$, Mo, Si, Mo_3Si	<20	0.5, 4.0, 0.3	1300, 175	α-$MoSi_2$	82	79.7[f]	14.4	3.2
3	β-$MoSi_2$, Mo, Si, Mo_3Si	<20	0.8, 0.5, 3.5	1400, 375	α-$MoSi_2$	38	97.9	16.3	3.2
3	β-$MoSi_2$, Mo, Si, Mo_3Si	<20	0.8, 1.0, 3.0	1400, 280	α-$MoSi_2$	91	90.7[f]	not tested	not tested

[a] Phases detected by XRD listed in order of decreasing X-ray intensities of the 100% reflection. [b] Powder crystallite size or compact grain size determined by XRD line broadening of $MoSi_2$ reflections. [c] Compact density expressed as a percentage of the density of single-crystal α-$MoSi_2$. [d] Vickers hardness number. [e] Fracture toughness. [f] Density determined by metalography.

mined using a precision microbalance and the Archimedes principle, or by metalography.

Results and Discussion

Preparation of $MoSi_2$ by Chlorine Transfer. $MoSi_2$ was prepared by heating solid mixtures of $MoCl_3$ and Si (eq 5). The first indications of reaction were noted at temperatures as low as ~400 °C, at which small, yellow crystals were observed to grow in the fused-silica tube just outside the furnace. X-ray diffraction patterns of this crystalline material established $MoCl_2$ (a yellow solid) as a major constituent phase, although several unidentified reflections were also present. $MoCl_2$ is not known to be volatile at 400 °C, which suggests operation of a vapor-phase-transport mechanism.

A few moments after a furnace temperature of 500 °C was reached, a vigorous reaction was initiated that proceeded to completion within a few seconds, with the liberation of a substantial amount of heat. The furnace thermocouple, which was not in contact with the reaction tube, registered a temperature elevation of ~50 °C. A large quantity of volatile byproduct was expelled during this process (along with small amounts of gray powder), which condensed as a colorless liquid in the tube outside the furnace. The liquid was identified to be $SiCl_4$ by ^{29}Si NMR. A dark gray powder was left in the reaction zone after the reaction, which consisted primarily of α-$MoSi_2$ possessing an average crystallite size exceeding 100 nm according to XRD line widths (Figure 2a). TEM images showed that the dimensions of most of the particles fell only slightly outside the nanometer regime in the 100−200 nm range. Most of these particles exhibited some degree of sintering with other particles (Figure S1 in the Supporting Information). EDS indicated that Cl elimination as $SiCl_4$ was essentially complete; less than 1 atom % Cl was detected in the product.

The rapidity of the highly exothermic process [$\Delta H_{298} = -62.0$ kcal/(mol of $MoSi_2$)] suggested that the maximum transient temperature achieved within the reaction mixture was high. We reasoned that smaller crystallite sizes, within the nanometer regime, might be obtained by moderating the reaction with a heat-absorbing diluent. For practical applications, this diluent could be a desired reinforcement phase, such as SiC. Our goal, however, was to generate monophasic *nano*-$MoSi_2$ for mechanical-properties testing. Consequently LiCl was initially used as the diluent material, which could be readily removed after the synthesis by sublimation at ~750 °C or by extraction with methanol.

A series of reactions was conducted (on the scale of a 2.5 g theoretical yield of $MoSi_2$) using increasing amounts of LiCl diluent. Parts b−g of Figure 2 show the XRD patterns obtained from the products of these reactions. As the LiCl:$MoCl_3$ molar ratio was increased from 0 to 10, the rate of the reactions diminished, as evidenced by the slowed evolution of $SiCl_4$ from the reaction zone. For molar ratios of ≥2.5 a few minutes was required for complete elimination of $SiCl_4$ (by visible inspection), and no temperature elevation was registered by the furnace thermocouple. As the reaction rate decreased,

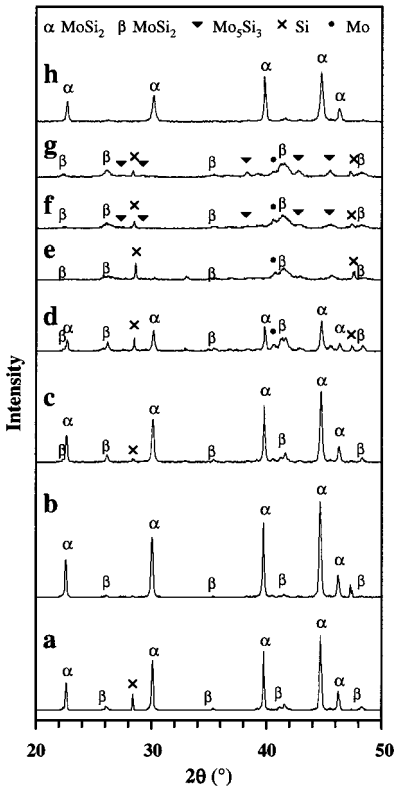

Figure 2. XRD patterns for powders obtained from eq 5 without and with added LiCl diluent. The LiCl:$MoCl_3$ ratio, annealing time at 500 °C, and major product (average grain size) for each reaction are as follows: (a) 0:1, 2 min, α-$MoSi_2$ (>100 nm); (b) 0.5:1, 2 min, α-$MoSi_2$ (~100 nm); (c) 1:1, 2 min, α-$MoSi_2$ (90 nm); (d) 1.5:1, 1 h, α-$MoSi_2$ (75 nm); (e) 2.5:1, 1 h, β-$MoSi_2$ (<10 nm); (f) 2.5:1, 36 h, β-$MoSi_2$ (<10 nm); (g) 10:1, 24 h, β-$MoSi_2$ (<10 nm). (h) Powder from Figure 2e heated at 900 °C for 12 h (α-$MoSi_2$, 54 nm). All patterns are for reactions conducted on a 2.5 g $MoSi_2$ scale except for that in Figure 2a, which corresponds to an 8 g scale. The phase Mo_3Si was not discerned in the specific cases included in this figure; however, Mo_3Si and β-$MoSi_2$ are difficult to distinguish in broadened patterns arising from small crystallites because of near coincidence of their major reflections. Reflections from $MoSi_3$ were often identified in the somewhat sharper patterns obtained from the products of larger-scale syntheses.

the $MoSi_2$ crystallite sizes became smaller (as determined by XRD line broadening) and the resultant $MoSi_2$ crystal structure switched from the α (tetragonal) to the metastable β (hexagonal) phase, which is known to be kinetically favored under some conditions.[23,29,30] However, the reactions also became increasingly less complete. XRD patterns of products obtained with the higher LiCl:$MoCl_3$ molar ratios contained, despite extended soak times at 500 °C (for up to 36 h), reflections for unreacted Si, metallic Mo, and some unidentified reflections not assignable to $MoSi_2$, Mo_5Si_3, or Mo_3Si.

Although reactions conducted with larger amounts of LiCl diluent were incomplete with respect to $MoSi_2$ formation, chlorine elimination did approach completion in these trials. EDS analysis of a product derived from a reaction employing a LiCl:$MoCl_3$ ratio of 2.5 contained only about 0.2 atom % chlorine, indicating that almost all of the chlorine had been removed as volatile byproducts. No chlorine-containing phases were observed in the solid products by XRD. Additionally, weight yields were consistent with the complete elimination of $SiCl_4$. These results were consistent with the visual observations that $SiCl_4$ elimination was completed within just a few minutes after initiation of the exothermic reaction.

Completion of $MoSi_2$ formation in the diluent-rich reactions occurred subsequently during removal of the LiCl by sublimation (750−900 °C, 10^{-3} Torr). The $MoSi_2$ material so obtained was nanocrystalline, despite the very large dimensions of the silicon particles in the mixtures prior to the sublimation step. Figure 2h shows the XRD pattern for a sample (LiCl:$MoCl_3$ = 2.5) after heating under vacuum for 12 h at 900 °C. The average grain size was calculated to be 54 nm from XRD line widths, which was consistent with the TEM images (Figure 3). The TEM images revealed relatively few particles having sizes ≥200 nm, and an abundance of 20 nm particles at the smallest end of the size distribution. Appreciable nanoparticle sintering was evident in this sample (Figure 3a). Sintered spherical aggregates that in some cases exceeded 1 μm were present (Figure S2 in the Supporting Information). These spherical aggregates may have formed to minimize interfacial contact between $MoSi_2$ and molten LiCl.

Reactions employing $ZnCl_2$ instead of LiCl as the diluent were investigated because $ZnCl_2$ sublimes rapidly at 500 °C and is highly soluble in methanol or ether, making it easier to remove than is LiCl. Very different results, however, were obtained. With a $ZnCl_2$:$MoCl_3$ ratio of only 0.625 the reaction proceeded much more slowly than at the highest LiCl:$MoCl_3$ ratios studied, and no abrupt exothermic ignition was observed. At a furnace temperature of 500 °C the reactant mixture retained the red color of $MoCl_3$ after 20 min, and $SiCl_4$ was observed to evolve very slowly. After the mixture was held at 500 °C for 14 h and the $ZnCl_2$ was removed by sublimation, XRD analysis indicated that formation of $MoSi_2$ was less complete than for any of the reactions employing LiCl as the diluent (Figure 4a). As above, these mixtures were converted to $MoSi_2$ with subsequent annealing. Figure 4c shows the XRD pattern obtained for a product annealed at 900 °C for which the average crystallite size (of α-$MoSi_2$) was determined to be 53 nm.

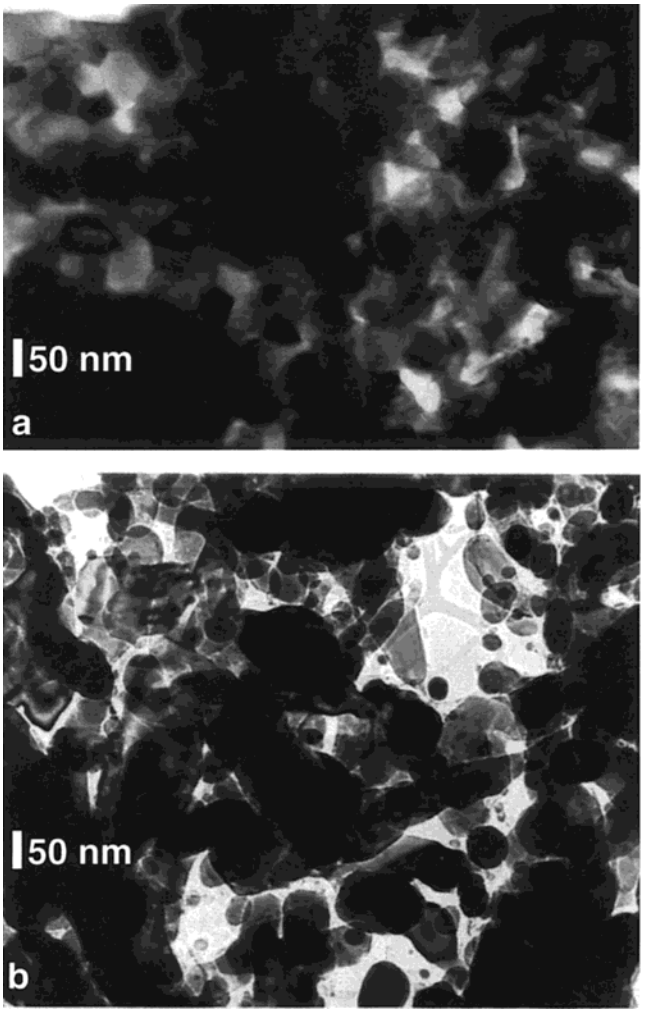

Figure 3. TEM images of a powder prepared with a LiCl diluent (LiCl:$MoCl_3$ ratio 2.5) and annealed for 12 h at 900 °C, which correspond to the XRD pattern in Figure 2h: (a) highly sintered $MoSi_2$ crystallites; (b) loose $MoSi_2$ crystallites present in the same sample.

The results establish that added diluents effectively moderate the exothermic reaction in eq 5, which both minimizes $MoSi_2$ grain growth and can preclude completion of the reaction. $ZnCl_2$:$MoCl_3$ ratios below 0.5 apparently moderate the reaction to a similar extent as does a LiCl:$MoCl_3$ ratio of 2.5, and therefore $ZnCl_2$ appears to be the more-effective diluent. We speculate that the lower melting point of $ZnCl_2$ (283 °C), as compared to that of LiCl (605 °C), may promote more-substantial wetting and passivation of the eq 5 reactant particles by $ZnCl_2$.

Generation of Mo. Our observation of Mo as an intermediate species when eq 5 was conducted with diluents (see Figures 2 and 4) suggested that nanocrystalline elemental Mo might be produced by a reaction analogous to that in eq 5. Consequently we investigated eq 6

$$4MoCl_3 + 3Si \rightarrow 4Mo + 3SiCl_4 \qquad (6)$$

$$[\Delta H_{298} = -25.3 \text{ kcal/(mol of Mo)}]$$

(29) Ma, E.; Pagán, J.; Cranford, G.; Atzmon, M. *J. Mater. Res.* **1993**, *8*, 1836.
(30) Liu, L.; Padella, F.; Guo, W.; Magini, M. *Acta Metall. Mater.* **1995**, *43*, 3755.

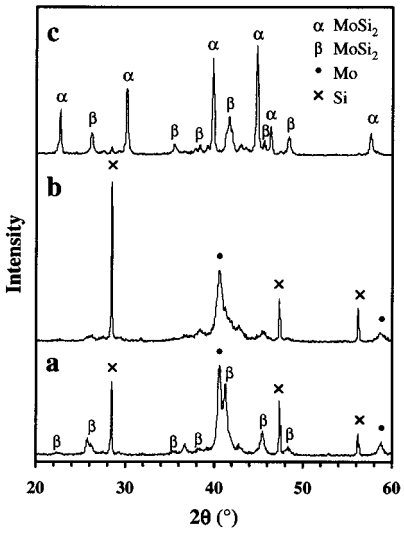

Figure 4. XRD patterns for powders obtained from eq 5 conducted with a $ZnCl_2$ diluent: (a) 0.625:1 $ZnCl_2/MoCl_3$, 500 °C for 14 h; (b) 2.5:1 $ZnCl_2/MoCl_3$, 500 °C for 14 h; (c) the product from (b) annealed at 900 °C for 12 h. The major products were Si, Mo, and β-$MoSi_2$ in (a), Si and Mo in (b), and α-$MoSi_2$ (53 nm average grain size) in (c).

(at 500 °C) in which the Si stoichiometry was just sufficient for reduction of $MoCl_3$ to elemental Mo, but not for conversion to $MoSi_2$. However, XRD and EDS analyses (Figure S3 in the Supporting Information) of the products revealed that some of the Si reactant was scavenged by Mo to form poorly crystallized silicide phases, resulting in incomplete reduction of $MoCl_x$, and a mixture of phases. This result is consistent with the lesser exothermicity of eq 6 in comparison to eq 5. Indeed, eq 6 does not appear to be a promising route to pure nanocrystalline Mo.

Powder Consolidation. Nanocrystalline $MoSi_2$ powders prepared in the presence of diluent (2.5:1 LiCl/$MoCl_3$) were consolidated by uniaxial hot pressing at 1300−1400 °C, a temperature slightly above the brittle-to-ductile transition temperature (BDTT) for conventional $MoSi_2$,[1] producing 13 mm diameter $MoSi_2$ disks (or cylinders) having thicknesses of 4.4−7.2 mm and masses of 3.75−6.00 g. Consolidation below the BDTT is impractical because the fracture stress of $MoSi_2$ is lower than its critical resolved shear stress for dislocation migration at such temperatures, meaning it will not deform plastically.[31,32] The high temperatures typically used for consolidation of conventional $MoSi_2$ (≥1600 °C) were avoided to minimize grain growth by diffusion-based consolidation mechanisms, such as Nabarro−Herring or Coble creep. The results of the consolidation trials are recorded in Table 1.

As shown in Table 1, compaction at 1400 °C and 375 MPa for as little as 30 min resulted in nearly complete densification (up to 97.9% of the theoretical density of $MoSi_2$). The nearly featureless SEM images of polished faces of the disks (Figure S4 in the Supporting Information) indicated the very low level of fine-scale porosity present in these compacts. The average $MoSi_2$ grain sizes determined from line widths in XRD patterns

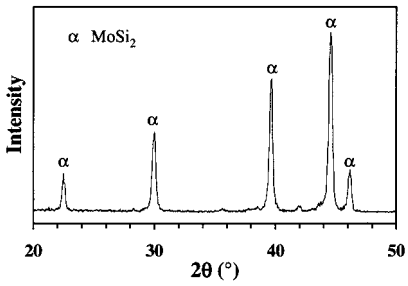

Figure 5. XRD pattern from a 95%-dense $MoSi_2$ compact that exhibits an average grain size of 32 nm. Additional data from this specimen are recorded in the second entry in Table 1, Figure 6, and Figure S4.

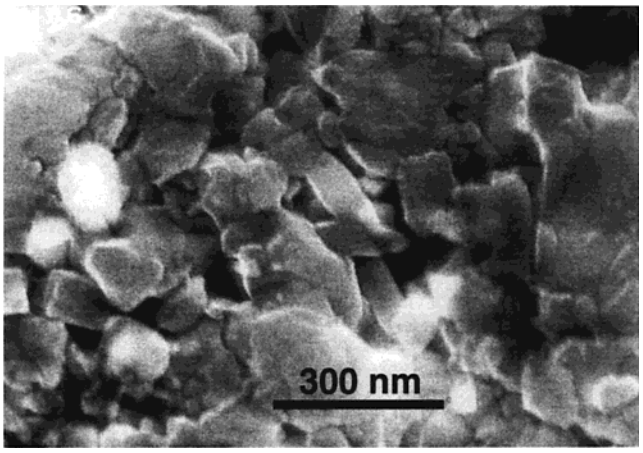

Figure 6. An SEM image of the polished and etched surface of a 95%-dense $MoSi_2$ compact, which exposes the nanoscale grain structure.

(Figure 5) of the highest-density disks (Table 1) were 32 and 38 nm. Accordingly, SEM images of polished and etched disk faces for these specimens revealed many fine grains around 30 nm in dimension, while the largest grains were only slightly larger than 100 nm in dimension (Figure 6). The grain sizes were on average smaller than those obtained by pressureless sintering of $MoSi_2$ powders at 900 °C (see above). All compacts produced in this study were phase-pure α-$MoSi_2$ according to XRD analysis (Figure 5). Only trace amounts of oxygen and carbon contaminants were detected by EDS.

Reducing the pressure and/or temperature of consolidation resulted in diminished densification and larger average grain sizes. A compact formed at 1300 °C and 175 MPa (Table 1) possessed a density of only 79.7% and an average grain size of 82 nm. Further, large interagglomerate pores were visible in this compact by SEM, an observation that may account for the larger grain sizes obtained. When high pressures are applied, interagglomerate pores are closed by interparticle sliding and rapid plastic deformation, hence obviating diffusional growth as a pore-closure mechanism. When the lower pressure was applied, the large pores were not rapidly closed and diffusional sintering was enabled, resulting in some grain growth.

No discernible enhancement in densification rate over coarse-grained $MoSi_2$ powders, which have been shown to condense to 93% of full density within 4 h at 1200 °C and 207 MPa,[33] was observed. This is in contrast to previous reports for densification rates of nanocrystalline materials in comparison to conventional, coarse-

(31) Umakoshi, Y.; Sakagami, T.; Hirano, T.; Yamane, T. *Acta Metall. Mater.* **1990**, *38*, 909.
(32) Aikin, R. *Scr. Metall.* **1992**, *26*, 1025.

grained counterparts,[34,35] but matches model predictions for the densification of nanocrystalline $MoSi_2$.[36] Enhanced rates have been attributed to greater diffusivities for the high-surface-area nanocrystalline materials. If plastic deformation is the dominant densification mechanism, however, as is predicted by the model studies, then enhanced rates are not expected. Nanoparticles have low dislocation densities, which should inhibit conventional plastic-deformation processes.[5] Furthermore, nanoparticles possess high surface area (and energy), leading to large interparticle attractions causing high frictional resistance.[36,37] At higher temperatures, where diffusion mechanisms are more important in densification, accelerated consolidation may indeed be observed for nanocrystalline $MoSi_2$ (but with simultaneous grain growth).

Mechanical Properties. Preliminary hardness and fracture toughness determinations of these nanocrystalline $MoSi_2$ materials were accomplished by microindentation and microindentation-induced cracking,[38] respectively (see Table 1). The compacts were not sufficiently large for standard tensile-strength testing or for three (or four) point bend testing to determine fracture toughness. Substantial enhancement in room-temperature hardness was observed for these nanocrystalline specimens in comparison to that of microcrystalline $MoSi_2$. The hardness of the densest specimen was 16.3 GPa, which is 75% greater than the 9.3 GPa reported for microcrystalline $MoSi_2$.[39] The less-dense nanocrystalline specimens exhibited somewhat lower hardness, as would be expected with increased porosity, but the values did not correlate with the determined densities. The lowest hardness value established in this study was 12.5 GPa, while the average was 14.6 GPa.

We did not observe significantly enhanced fracture toughness for nanocrystalline $MoSi_2$, although the higher indentation loads required to induce cracking compared to those of microcrystalline samples likely indicate some enhancement in toughness. The average calculated toughness was 3.8 MPa $m^{1/2}$, and the maximum value was 4.8 MPa $m^{1/2}$, while the toughness of microcrystalline $MoSi_2$ has been reported as 3.0 MPa $m^{1/2}$.[40] These values were calculated using the elastic modulus for single-crystal $MoSi_2$ (440 GPa),[41] but the modulus for nanocrystalline $MoSi_2$ may be significantly higher,[21] which would yield higher toughness values.

The higher fracture-toughness values were exhibited by two of the rapidly cooled consolidates, suggesting (but not requiring) a toughening mechanism consisting of stress relief of a growing crack at voids or microcracks. (A third rapidly cooled consolidate exhibited a low fracture toughness presumably because of its low density.) The dense consolidate that was slowly cooled was probably microcrack free, resulting in higher hardness but lower toughness.

The mechanical properties determined here are in contrast to those reported for nanocrystalline $MoSi_2$ prepared by mechanical attrition.[21] A maximum hardness of only 10.43 GPa was established, but fracture toughness up to 6.91 MPa $m^{1/2}$ was reported. Those materials were quite different from those discussed herein, however. Average grain sizes in the mechanically attrited samples were comparable (38−54 nm) to those observed here, but densities were much lower (≤92.8%), and large interagglomerate pores were present as a result of the difficulty of consolidating the large agglomerates obtained by milling.[27] Further, the mechanically attrited samples contained substantial oxygen and nitrogen impurities resulting from adventitious air exposure during milling in liquid N_2. Thus, the high toughness of the mechanically attrited samples may be due to impurity toughening in addition to void/microcrack toughening. The disparity between the results from nanocrystalline specimens produced by mechanical attrition and those reported here attests to the significant influence that processing strategies and resultant product microstructures and impurity compositions can have upon the mechanical properties of nanocrystalline materials.

Chlorine Transfer as a General Strategy for Preparing Intermetallic or Ceramic Materials. Formation of $SiCl_4$ provides a sufficient thermodynamic driving force to allow many transition-metal halides to undergo chlorine-transfer reactions analogous to that in eq 5. However, the exothermicity of few such reactions approaches that of eq 5 for the formation of $MoSi_2$. One reaction having a lesser enthalpic driving force was attempted for the preparation of VSi_2 (eq 7). The

$$4VCl_3 + 11Si \rightarrow 4VSi_2 + 3SiCl_4 \qquad (7)$$

reaction was not observed to be initiated until 600 °C, and at this temperature only trace amounts of VSi_2 were formed. The material was further annealed at 900 °C to complete VSi_2 formation, but the VSi_2 produced was microcrystalline rather than nanocrystalline. The high temperature required to complete this reaction is similar to those reported by Parkin for related metathesis-like reactions that generate metal silicide phases.[42]

The chlorine-transfer strategy appears to be even less promising for the more-desirable refractory silicides Ti_5Si_3 and Zr_5Si_3, because the starting titanium and zirconium halides are too stable, making the chlorine-transfer reactions endothermic. We attempted such reactions, and they were indeed unsuccessful. Therefore, the chlorine-transfer strategy is unlikely to provide a general route to a variety of nanocrystalline silicides.

Consideration was given to the prospects for preparing other intermetallics or ceramics, such as transition-metal borides, aluminides, carbides, germanides, phosphides, etc., by similar chlorine-transfer reactions. Because the heats of formation of most of these product compounds are not very great compared to those of the

(33) Suryanarayanan, R.; Sastry, S. M. L.; Jerina, K. L. *Acta Metall. Mater.* **1994**, *42*, 3742.
(34) Gronsky, R.; Hahn, H.; Ramasamy, S.; Siegel, R. W.; Ting, L.; Zongquan, L. *J. Mater. Res.* **1988**, *3*, 1367.
(35) Liao, Y. X.; Mayo, M. J.; Nix, W. D.; Siegel, R. W. *J. Mater. Res.* **1992**, *7*, 973.
(36) Suryanarayanan Iyer, R.; Sastry, S. M. L. *Acta Mater.* **1999**, *47*, 3079.
(37) Suryanarayanan, R. D. Sc. Dissertation, Washington University, St. Louis, MO, 1996; p 183.
(38) Antis, G. R.; Chantikul, P.; Lawn, B. R.; Marshall, D. B. *J. Am. Ceram. Soc.* **1981**, *64*, 533.
(39) Bhattacharya, A. K.; Petrovic, J. J. *J. Am. Ceram. Soc.* **1991**, *74*, 2700.
(40) Unal, O.; Petrovic, J. J.; Mitchell, T. E. *J. Mater. Res.* **1993**, *8*, 626.
(41) Nakamura, M.; Matsumoto, S.; Hirano, T. *J. Mater. Sci.* **1990**, *25*, 3309.
(42) Parkin, I. P. *Chem. Soc. Rev.* **1996**, *25*, 199−207.

halide reactants, the byproduct halide must be very stable to provide a sufficient enthalpic driving force for spontaneous ignition. Of the byproduct halides, only the heat of formation of $AlCl_3$ (−139.4 kcal/mol) is comparable to that of $SiCl_4$ (−157.0 kcal/mol) on a per-mole-of-chlorine basis. The chlorine-transfer strategy may be suitable, then, for the preparation of aluminide intermetallics. Several reports in the Russian literature appear to confirm this expectation.[43−47]

Acknowledgment. This work was supported by AFOSR Grant No. F49620-93-1-0131.

Supporting Information Available: Figures S1−S4 showing the TEM image of $MoSi_2$ obtained from eq 5, TEM images of a powder prepared with a LiCl diluent, an XRD pattern of a powder obtained from eq 6, and an SEM image of a 95%-dense $MoSi_2$ compact (PDF). This material is available free of charge via the Internet at http://pubs.acs.org.

CM010267C

(43) Zviadadze, G. N.; Chkhikvadze, N. V. *Soobshch. Akad. Nauk Gruz. SSR* **1975**, *77*, 105.
(44) Zviadadze, G. N.; Chkhikvadze, N. V.; Pulariani, Yu. I. *Soobshch. Akad. Nauk Gruz. SSR* **1975**, *77*, 393.
(45) Zviadadze, G. N.; Shengeliya, O. V.; Gigineishvili, A. A. *Soobshch. Akad. Nauk Gruz. SSR* **1975**, *77*, 649.
(46) Zviadadze, G. N.; Shengeliya, O. V.; Gigineishvili, A. A. *Soobshch. Akad. Nauk Gruz. SSR* **1975**, *78*, 141.
(47) Gazizov, R. K.; Lebedev, V. A.; Nichkov, I. F.; Poyarkov, A. M.; Raspopin, S. P. *Izv. Vyssh. Uchebn. Zaved., Tsvetn. Metall.* **1975**, 144.